The Colicin E3 Outer Membrane Translocon: Immunity Protein Release Allows Interaction of the Cytotoxic Domain with OmpF Porin†

Stanislav D. Zakharov,‡,§ Mariya V. Zhalnina,‡ Onkar Sharma,‡ and William A. Cramer*,‡

Department of Biological Sciences, Purdue University, West Lafayette, Indiana 47907, and Institute of Basic Biological Problems, Russian Academy of Sciences, Pushchino, Moscow Region 140290, Russian Federation

Received April 10, 2006; Revised Manuscript Received June 8, 2006

ABSTRACT: The crystal structure previously obtained for the complex of BtuB and the receptor binding domain of colicin E3 forms a basis for further analysis of the mechanism of colicin import through the bacterial outer membrane. Together with genetic analysis and studies on colicin occlusion of OmpF channels, this implied a colicin translocon consisting of BtuB and OmpF that would transfer the C-terminal cytotoxic domain (C96) of colicin E3 through the *Escherichia coli* outer membrane. This model does not, however, explain how the colicin attains the unfolded conformation necessary for transfer. Such a conformation change would require removal of the immunity (Imm) protein, which is bound tightly in a complex with the folded colicin E3. In the present study, it was possible to obtain reversible removal of Imm in vitro in a single column chromatography step without colicin denaturation. This resulted in a mostly unordered secondary structure of the cytotoxic domain and a large decrease in stability, which was also found in the receptor binding domain. These structure changes were documented by near- and far-UV circular dichroism and intrinsic tryptophan fluorescence. Reconstitution of Imm in a complex with C96 or colicin E3 restored the native structure. C96 depleted of Imm, in contrast to the native complex with Imm, efficiently occluded OmpF channels, implying that the presence of tightly bound Imm prevents its unfolding and utilization of the OmpF porin for subsequent import of the cytotoxic domain.

Bactericidal colicins exert their lethal effect on susceptible *Escherichia coli* strains through nuclease action on DNA, rRNA, or tRNA, formation of ion-conductive channels in cytoplasmic membranes, or inhibition of murein synthesis (for reviews, see refs *3*−*6*). These highly specialized toxins contain three definable domains [e.g., colicins Ia (*7*), E3 (Figure 1A; ref *8*)]. The 96-residue C-terminal domain of colicin E3 (C96)[1] is responsible for cytotoxicity and the central receptor binding (R135) and N-terminal translocation (T) domains for receptor recognition and import of the colicin to the cellular target. Colicin entry into the bacterial cell provides a model for studies of protein import across the double membrane system of Gram-negative bacteria, for which the cytotoxicity of the imported colicin is a simple marker (*6*, *9*).

A translocon model for cellular import of colicin E3 (colE3), based on the X-ray structure of the BtuB receptor with the bound R-domain (R135) of colE3 (*10*), proposed that the elongate colE3, bound to BtuB, can seek, locate, and form a complex with another outer membrane protein which, from previous genetic studies (*11*), was proposed to be the porin, OmpF. Among the different membrane translocon systems for protein import (*12*, *13*), studies on colicin import are presently unique in being able to utilize the insight gained from a high-resolution structure of a domain (R135) of the imported protein with the integral membrane (BtuB) receptor (*10*).

The existence of an outer membrane protein complex between colicin E3, BtuB, and OmpF has been demonstrated (*14*). The pores of the OmpF trimer [cross section, 7 × 11 Å (*15*, *16*)] could support insertion of the N-terminal translocation domain and passage of the C-terminal domain responsible for cytotoxicity, but only if these polypeptide domains are mostly unfolded. The colicins with endonuclease activity and their cognate immunity (Imm) proteins are coexpressed in host cells and exported as a tight complex (*17*−*19*) that is preserved during purification (*20*). Considering the bridging position of Imm between T- and C-domains in the colicin structure (Figure 1A), and its extremely high binding affinity, unfolding of the colicin must require removal of Imm from this tight complex (*2*, *9*).

Direct interaction of colE3 and its domains with OmpF, studied with planar bilayers containing incorporated OmpF, showed that colE3 can interact with OmpF through the disordered N-terminal segment of the T-domain, resulting in occlusion of OmpF channels (*21*). In these studies, the complex of the cytotoxic domain, C96, with Imm did not occlude the OmpF channels. This implied either that C96

† These studies were supported by a grant from the NIH (GM18457) and the Henry Koffler Professorship (W.A.C.).

* Corresponding author. Phone: 765-494-4956. Fax: 765-496-1189. E-mail: waclab@purdue.edu.

‡ Purdue University.

§ Russian Academy of Sciences.

[1] Abbreviations: C96, 96-residue C-terminal cytotoxic domain; CD, circular dichroism; colE3, colicin E3; colE3Imm, complex of colicin E3 with Imm; Gdn-HCl, guanidine hydrochloride; ϵ_M, molar extinction coefficient; Imm, immunity protein; P_i, inorganic phosphate; R135, RC, T-domain, colicin E3 receptor-binding, receptor-activity, and N-terminal translocation domain; RMSD, root mean square deviation; Trp, tryptophan; T83, N-terminal segment of the translocation domain, residues 1−83; T_m, temperature midpoint of thermal melting transition.

10.1021/bi060694+ CCC: $33.50
Published on Web 08/08/2006

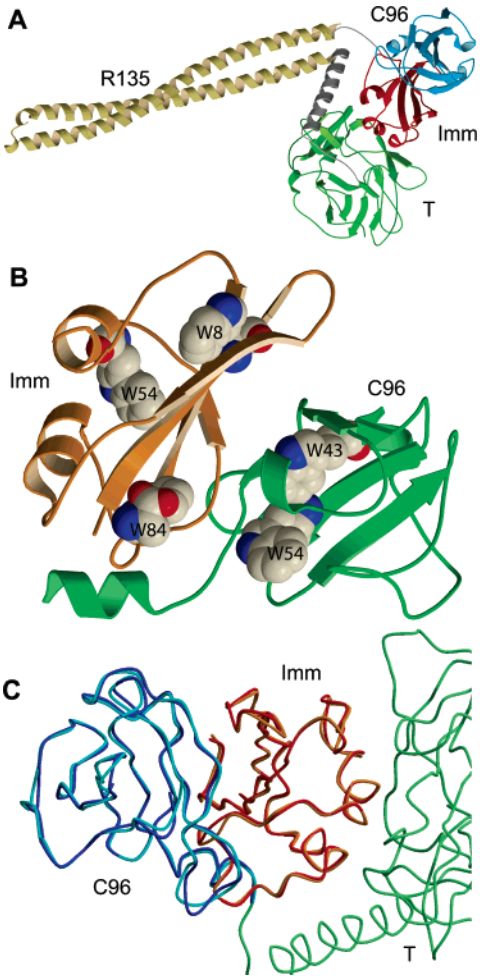

FIGURE 1: (A) Crystal structure of colicin E3 complexed with Imm. Colicin E3 N-terminal translocation (T), central receptor-binding (R135), and C-terminal cytotoxic (C96) domains, determined by crystal structure analysis (*8*), are shown in green, gold, and blue, respectively. Immunity protein (Imm) is in red. (B) Position of Trp side chains in C96 and Imm. Ribbon diagram of the C96Imm complex with C96 and Imm shown in green and orange, respectively. W43 and W54 in C96 correspond to residues 498 and 509, respectively, in intact colE3. (C) Superposition of backbones of the cytotoxic domain and Imm in intact colicin E3 (*8*) and the complex of the recombinant cytotoxic domain with Imm (*32*). C96 and Imm in the intact colicin complex are shown in cyan and orange and in the truncated C96Imm complex in blue and red, respectively. The remainder of the intact colicin is shown in green. The root mean square deviation for backbone atoms of the entire Imm and C96 (residues 455−551) is 0.36 and 0.52 Å, respectively.

does not use OmpF for its translocation into the periplasm or that the C96 structure must undergo a conformational change to expose its hidden OmpF recognition sites and/or to sterically allow insertion−passage into/through OmpF.

Previously, it appeared that Imm removal from colicin E3 required colicin denaturation (*2*, *20*, *22*), limiting studies of the interaction of colicin and its individual domains with Imm. In the present studies, a simple chromatographic method is demonstrated for Imm release in vitro that does not require protein denaturation. It is shown that Imm release results in a decrease of structure stability and extensive conformational change of Imm-free colE3, resulting in a mostly disordered C-terminal cytotoxic domain, although it does not have a large effect on cytotoxicity. The Imm-free cytotoxic domain is shown to occlude OmpF channels incorporated into planar bilayer membranes, implying that the cytotoxic domain exposes OmpF recognition sites upon Imm release and can insert into the lumen of OmpF channels. It is proposed that the action of the outer membrane translocon for colicin E3 import results in translocation of its C-terminal cytotoxic domain across the bacterial outer membrane through the OmpF porin.

EXPERIMENTAL PROCEDURES

Colicin Purification. The ColE3Imm complex, immunity protein, and colE3 fragments were expressed in IPTG-induced BL21(DE3) cells transformed with the respective plasmids. ColE3Imm, R135, and T83 (N-terminal fragment of colE3, residues 1−83) were cloned into pET41b plasmid (pET21b for R135) between the *Nde*I and *Xho*I restriction sites, allowing expression of cloned polypeptides with the C-terminal His tag (His_8 tag at the C-terminus of Imm in the colE3Imm complex). The C96Imm complex was expressed in BL21(DE3) cells transformed with plasmid pKSJ188 kindly provided by K. Jakes (Albert Einstein College of Medicine) with a gene construct for the N-terminal His_6 tag and an SSGLVPRGSHM linker to the C96 polypeptide. The T-domain (residues 84−315) was also expressed in BL21(DE3) transformed with plasmid pBAD-NtE3 (residues 84−315) kindly provided by E. Bouveret (CNRS, Marseille, France) with an N-terminal His tag. The polypeptides were purified on a Ni^{2+}-precharged HisTrap 5 mL column (Amersham Biosciences).

To obtain Imm-free C96, purified C96Imm with the N-terminal His_6 tag in C96 was loaded on a Ni^{2+}-precharged column. Imm was eluted with 2−3 column volumes of 6 M Gdn-HCl, followed by 5 volumes of 10 mM Tris, pH 8.0, and 5 mM imidazole. Imm-free C96 was eluted from the column with 0.5 M imidazole and 10 mM Tris, pH 8.0.

Protein Concentration. Concentrations of colE3 ($\epsilon_M \approx$ 57 410), Imm ($\epsilon_M \approx$ 22 460), colE3Imm ($\epsilon_M \approx$ 79 870), C96 ($\epsilon_M \approx$ 18 450), C96Imm ($\epsilon_M \approx$ 40 910), and T83 ($\epsilon_M \approx$ 16 500) were determined spectrophotometrically using the absorbance at 280 nm after subtraction of background light scattering. The light scattering at 280 nm was extrapolated from the sample absorbance in the spectral range 320−400 nm where colE3 and Imm do not have absorbance.

Removal of Imm from the Complex with Colicin E3 by Anion-Exchange Chromatography. Binding of purified His-tagged colE3Imm to the high-affinity anion-exchange resin (HiTrap Q, 5 mL column; Amersham Biosciences) resulted in the elution of a fraction of colE3 without Imm (Figure 2). ColE3Imm was applied to the Q column equilibrated with 5 mM Tris, pH 8.0. The column was washed with 4 volumes of Tris buffer, followed by 10 volumes of a linear salt gradient (0−0.8 M NaCl) in the same buffer. Imm-free colE3 was released at the start of the salt concentration gradient, followed by a colE3Imm complex, whereas the Imm was eluted at a much higher salt concentration (Figure 2, inset). Complete removal of Imm from the colE3Imm complex can be achieved using a 20 mL HiPrep Q column. A similar chromatographic separation was obtained with the wild-type colE3Imm complex, implying that dissociation of Imm from the complex was not caused by the presence of the His_8 tag in Imm.

Cytotoxicity. Colicin cytotoxicity was assayed by a microbiological spot test on agar plates using *E. coli* K17

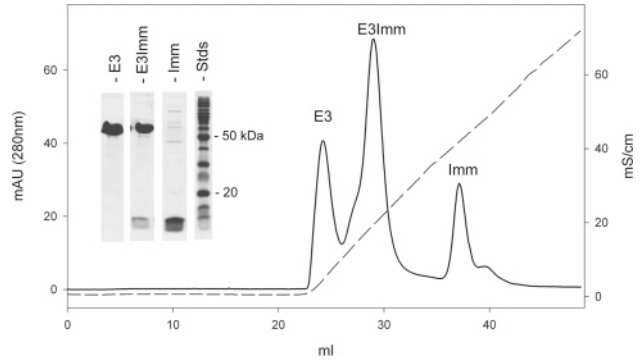

FIGURE 2: Separation of Imm and colicin E3 using anion-exchange chromatography. Colicin E3, in its native state, with bound Imm (0.6 mg of total protein) was purified as described in Experimental Procedures. Colicin E3 without Imm, Imm complex with colicin, and Imm alone were eluted from the column at salt concentrations corresponding to a conductance of 4.5, 19.5, and 42 mS/cm, respectively. Solid and dashed lines describe absorbance at 280 nm and conductance in the eluate, respectively. (Inset) SDS electrophoresis of eluted fractions: colE3, colE3Imm complex, Imm, and protein molecular mass standards.

indicator cells. Aliquots of serial dilutions of colicins (20 μL) were applied to a fresh bacterial lawn on plates with 1.4% agar prepared in LB medium. Plates were incubated at 37 °C until a dense lawn appeared with clear spots where the colicin activity was sufficient for it to exert a cytotoxic effect.

Circular Dichroism. The far- and near-UV circular dichroism (CD) spectral measurements were carried out with a J-810 spectropolarimeter (JASCO) equipped with Peltier temperature control. Spectra were measured at 20 °C, using cuvettes with an optical path length of 0.1 and 10 mm, respectively, for far- and near-UV CD measurements. Samples were dissolved in 10 mM Tris, pH 8.0, and 0.1 M NaCl. CD analysis of thermal denaturation of colicin domains was performed at 222 nm in a stirred cuvette having an optical path length of 10 mm, with a rate of temperature change of 30 °C/h.

Intrinsic Protein Fluorescence Emission Spectra. Spectral measurements were carried out with a FluoroMax-3 spectrofluorometer (Horiba, Jobin Yvon) equipped with a Peltier temperature controller, LFI-3751 (Wavelength Electronics). Excitation spectra of the intrinsic fluorescence of C96 and Imm assayed at 320 and 340 nm, respectively, were measured over a wavelength range of 250−310 nm at 20 °C. In both cases, the excitation spectra have a maximum at 282 nm. To minimize the contribution of tyrosines in the tryptophan emission spectra (305−400 nm; bandwidth, 2 nm), the fluorescence was excited at 295 nm (bandwidth, 2 nm). To test the thermal stability of proteins, the temperature dependence of Trp fluorescence spectra was measured in the range 2−80 °C with temperature steps of 2 °C, an equilibration time of 2 min, and an accuracy of ±0.4 °C.

OmpF Channel Measurements in Planar Bilayers. Planar bilayer membranes were formed on a 0.2 mm diameter aperture in a partition that separates two 4 mL compartments of the experimental setup, using a 1:1 (mol/mol) mixture of the two lipids, dioleoylphosphatidylcholine and dioleoylphosphatidylethanolamine (10 mg/mL) in *n*-decane, applied by a brush technique (*23*). The aqueous solution in both compartments consisted of 5 mM KP_i, pH 7.0, and 0.1 M KCl. OmpF, 0.1−2 μL of a 0.1−10 ng/mL solution in 1% octyl-POE, was added to the *cis*-compartment, and the solution was stirred until channels appeared. The transmembrane current was measured in the voltage-clamp mode with Ag/AgCl electrodes, using a BC-525C amplifier (Warner Instruments, Hamden, CT). The sign of the transmembrane potential is specified for the *cis*-side of the membrane.

RESULTS

I. Release of Immunity Protein in Vitro. Electrostatic interactions between the basic colE3 (pI = 9.3) and the acidic cognate Imm protein (pI = 4.2) contribute to the high affinity [($K_d \approx 10^{-14}$ M (*2*)] between these proteins. An apparent requirement of denaturing conditions (6 M Gdn-HCl) for release of Imm from the native colE3Imm complex (*2*, *22*) is consistent with this high affinity. It was found in the present studies that Imm could be separated from the colicin molecule in a native state on an anion-exchange (HiTrap Q) column (Figure 2). Interaction of Imm at low ionic strength with the strong anion-exchange column (ionic capacity, ~0.22 mmol/mL) allows its separation from the colicin and elution of native Imm-free colE3 from the column (Figure 2). Chromatography of colE3Imm on a weak anion-exchange HiPrep 16/10 DEAE column (ionic capacity, ~0.13 mmol/mL), previously employed (*24*, *25*), or the binding of the complex at higher ionic strength (>20 mM NaCl) did not release Imm.

The minimal concentration of Imm-free colE3 at which it was cytotoxic toward susceptible *E. coli*, measured by a "spot" test (see Experimental Procedures), was slightly (3−5 times) larger than that (100 pM) required for cytotoxicity of the colE3Imm complex. Reconstitution of the complex by addition of Imm to Imm-free colE3 restored the effective cytotoxic concentration to the level of native colE3Imm (data not shown). The small decrease in cytotoxicity of Imm-free colE3 may be explained by reversible dimerization of the Imm-free colicin (*26*).

II. Occlusion of OmpF Channels by the Cytotoxic Domain of Colicin E3. It was previously shown (*21*) that the 58 kDa colicin E3 molecule can efficiently (concentration, 10 nM) and specifically occlude the large well-characterized ion channels of OmpF incorporated into planar bilayers (*15*, *27*, *28*). OmpF is occluded also by colicins A and N, but not by the TolC-dependent colicin E1, and TolC is occluded by colicin E1, but not by colicin A, E3, or N (*21*). From these experiments, previous genetic analyses (*11*), and isolation of a BtuB−colE3Imm−OmpF complex (*14*), it was inferred that OmpF is utilized by colicin E3 to cross the outer membrane. The N-terminal segment of the translocation domain was required for this interaction (*21*). RC- and C-domains, each complexed with Imm, did not have any effect on the conductance of OmpF channels. This posed a problem, as the cytotoxic C-domain must be imported. Because import of the endoribonucleolytic colicins is coupled to release of the immunity protein into the extracellular medium (*19*) (Zakharov et al., 2006),[2] the interaction of the cytotoxic domain with OmpF was reexamined using the isolated Imm-depleted cytotoxic domain.

[2] 50th Annual Biophysical Society Meeting, Salt Lake City, UT, Feb 18−22, 2006, Abstracts 2509 and 2510.

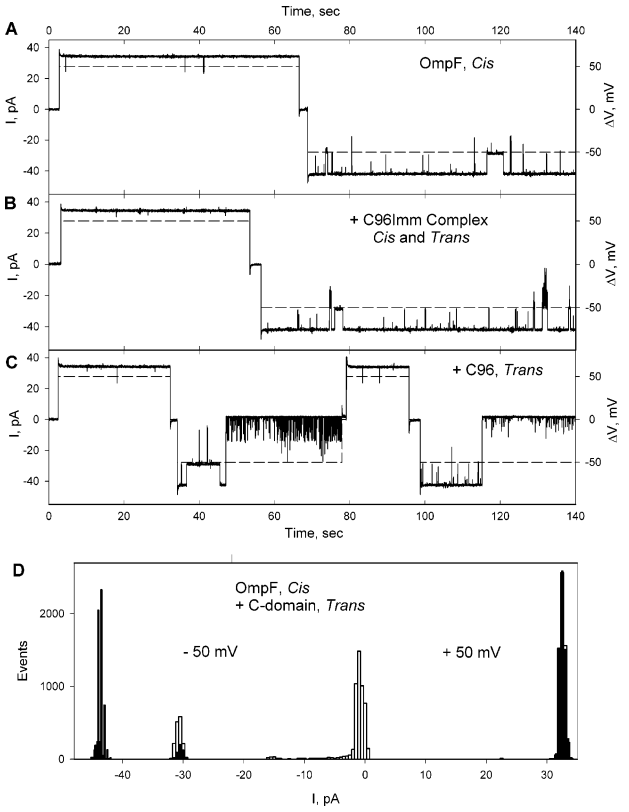

FIGURE 3: Occlusion of OmpF channels by the Imm-free cytotoxic domain. (A) A planar bilayer membrane was incubated with OmpF (12 pg/mL) in the *cis*-compartment. After channels were observed, unbound OmpF was removed by perfusion of the chamber to prevent incorporation of new channels. The trans-membrane current was measured upon the application of trans-membrane potentials (dashed), +50 or −50 mV (the sign of the potential is that of the *cis*-compartment). (B) C96Imm complex (0.5 nmol/mL) added to *cis* and *trans* sides. (C) Imm-free C96 (100 pmol/mL) was added to the *trans*-compartment. Complete occlusion is observed at −50 mV. OmpF channels open again at +50 mV. (D) Histograms of trans-membrane currents for records in A (filled) columns and C (open) are shown. Representative 50 s segments of records taken 10 s after imposing the trans-membrane potential were used for the histograms. Buffer: 5 mM Tris, pH 7.2, and 0.1 M KCl.

Incorporation of OmpF into the planar lipid bilayer resulted in the formation of slightly asymmetric ion channels (all three channels open; trans-membrane current, +34 and −42 pA, respectively, with *cis*-positive and negative potentials; Figure 3A,D). Imm alone (not shown) or the C96Imm complex, 0.5 nmol/mL, added from either side of the planar bilayer membrane, did not affect the conductance of OmpF channels (Figure 3B). Imm-free C96 added (100 pmol/mL) from the *trans*-side resulted in the reversible closing of all three OmpF channels at a *cis*-negative trans-membrane potential. This is shown in the trace of the channel current between 45 and 80 s (Figure 3C) and a histogram of the distribution of currents before and after *trans*-side addition of C96 (Figure 3D). Channels opened at a positive potential. Addition of Imm-free C96 from the *cis*-side of the membrane did not affect OmpF channels (not shown). In this respect, Imm-free C96 behaved like intact colicin E3 and its T-domain (*21*), suggesting that the cytotoxic domain of colicin E3, possibly guided by the T-domain, uses OmpF to cross the outer membrane to enter the periplasm. Thus, the presence of tightly bound Imm prevents unfolding of the C-domain and utilization of the OmpF porin for its import.

The presence of the N-terminal His_6 tag in Imm-free C96 did not prevent its occlusion of OmpF channels in contrast to occlusion by the T-domain, which is abolished in colE3Imm that has an N-terminal His_6 tag (not shown). This suggests that the C-terminus, which has a more basic character than the N-terminus, may be responsible for the interaction of C96 with OmpF.

III. Disordered Secondary Structure of Imm-free C96. To analyze the mechanism of Imm prevention of the C96 interaction with OmpF, structure changes in the cytotoxic domain and in colE3 upon Imm release were studied using circular dichroism and intrinsic Trp fluorescence spectroscopy. To evaluate the stability and the extent of unfolding of C96 upon Imm release, CD spectra were measured as a function of temperature and were compared with spectra of intrinsically disordered polypeptide T83, the Gly-rich 83-residue N-terminal segment of the colicin E3 T-domain (*29*, *30*).

According to an analysis of structures previously determined crystallographically (*31*, *32*), C96 (in complex with Imm) and Imm (in complex with C96 or alone) contain a similar amount of α-helix and *β*-strand structure [16% and 24% in C96 and 20% and 30% in Imm, respectively, according to helix and sheet assignment in C96Imm (*32*)]. C96 and Imm also have a similar content of residues (2 Trp and 5 Tyr in C96; 3 Trp and 4 Tyr in Imm), which allow near-UV CD spectra to report on their tertiary structure.

The CD spectrum of Imm (Figure 4A, blue), with a minimum at 205 nm and a maximum at 192 nm, shows the presence of *β*-strand and α-helical structures (*33*). In contrast, the spectrum of Imm-free C96 (Figure 4A, red) displays a minimum between 190 and 200 nm that is characteristic for unordered polypeptides (*34*). The spectrum of the C96 CD signal below 215 nm is similar to that of T83 (Figure 4A, brown), which is disordered and not seen in the X-ray structure (*8*). There is no indication in the far-UV CD spectra of a significant content of α-helix and *β*-strand in C96 and T83. The similarity of these spectra, except for a spectral band centered at 228 nm, which does not arise from secondary structure, implies that Imm-free C96 has a small content of secondary structure compared to C96 in the C96Imm complex (Figure 4A, green). The 228 nm band in the spectra of C96 and the C96Imm complex is associated with aromatic side chains of C96 (see section IV).

To detect the relative order of secondary structures through their melting, far-UV CD spectra of T83, Imm, and C96 were measured from 20 to 80 °C, starting at 20 °C (Figure 4B−D). The absence of α-helical and *β*-strand structures in the intrinsically disordered T83, discussed above, is consistent with the virtual absence of a temperature dependence of changes in wavelength and amplitude of its 198 nm minimum (Figure 4B). The CD spectra of Imm also did not change in the temperature range 20−40 °C but between 40 and 60 °C showed a spectral shift to shorter wavelength and shift of the local minimum from 205 to 201 nm (Figure 4C), spectral changes expected for the transition of α-helix and/or *β*-strand structures to random coil (*33*). In contrast, the CD spectrum of C96, with a minimum at 196 nm at 20 °C, showed only small temperature-dependent changes related to melting of the secondary structure (Figure 4D). The similarity between C96 and T83 of the temperature dependence of spectral changes below 210 nm implies an absence or greatly

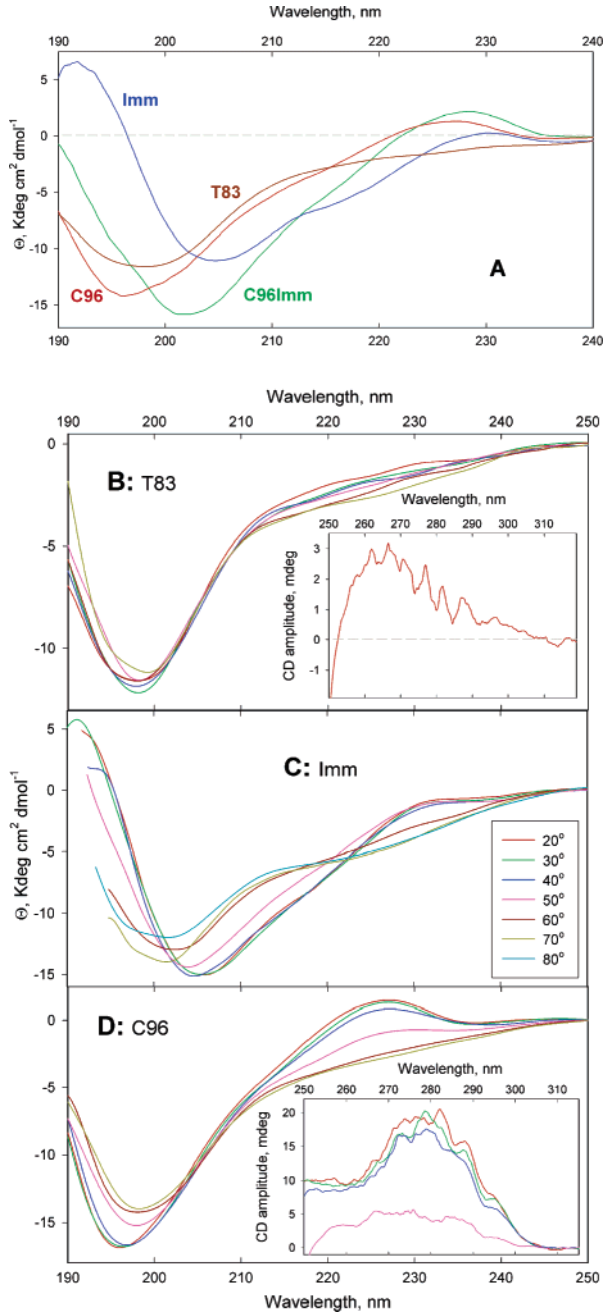

FIGURE 4: Imm release results in loss of α-helical and *β*-strand secondary structure of C96. (A) Far-UV CD spectra of C96 (red), Imm (blue), C96Imm complex (green), and T83 (brown) at 25 °C. Spectra were measured in a cell with an optical path length of 0.1 mm. Buffer: 10 mM Tris, pH 8.0, and 0.1 M NaCl. (B) Far-UV CD spectra of T83 (10 *μ*M) at 20−70 °C. (Inset) The near-UV CD spectrum of T83 (145 *μ*M) at 20 °C. (C) Far-UV CD spectra of Imm (10 *μ*M) at 20−80 °C. (D) Far-UV CD spectra of C96 (10 *μ*M) at 20−70 °C. (Inset) The near-UV CD spectra of C96 (112 *μ*M) at 20−50 °C. Buffer for (B)−(D): 20 mM NaP_i, pH 7.2. The optical path length for the far- and near-UV spectra was 1 and 10 mm, respectively. Specific ellipticity, Θ, is calculated per mole of amino acid residues.

decreased content of α-helix and *β*-strand in Imm-free C96 compared to C96 in the complex with Imm.

IV. Imm-free C96 Has a Hydrophobic Core. The CD signals of C96 between 210 and 240 nm decreased and vanished between 40 and 60 °C (Figure 4D). The parallel decrease in amplitude of the C96 CD maximum at 228 nm (Figure 4D), together with the CD spectrum in the near-UV region (Figure 4D inset), shows that the 228 nm band arises from aromatic residues of C96. Inducible CD signals between 220 and 240 nm, arising from Trp and Tyr residues constrained by tertiary structure packing, are observable in the far-UV CD spectra of polypeptides having a small content of α-helix (*35*, *36*). W498F and W509F mutations in C96 decreased and abolished, respectively, the maximum at 228 nm (not shown).[3] W498 and W509 of C96 in the C96Imm complex are not solvent-accessible (Table 1). The position of a Trp fluorescence emission maximum at $\lambda_{em} = 320$ nm (Figure 5A, inset) implies that, despite the small amplitude of this spectrum, W498 and W509 are in a hydrophobic environment, and it can be concluded that Imm-free C96 has a hydrophobic core. In fact, both W498 and W509 are in a such core, because the single Trp mutants of C96, W498F and W509F, have fluorescence emission maximum at 325 and 320 nm, respectively, and thermal denaturation of each results in a shift of the maximum to ∼355 nm (not shown).

Table 1: Solvent-Accessible Area of Trp and Tyr Side Chains of C96 and Imm in the C96Imm Complex[a]

		C96Imm complex (1E44)[b]		
protein	residue	shielded, Å^2	Imm or C96 removed, Å^2	Imm (3EIP),[c] Å^2
C96	W498	12	12	
	W509	18	19	
	Y460	72	145	
	Y464	34	117	
	Y507	12	12	
	Y519	2	2	
	Y550	49	95	
Imm	W8	21	21	25
	W54	22	22	25
	W84	60	95	124
	Y21	50	95	98
	Y61	101	101	81
	Y73	6	6	2
	Y79	6	74	77

[a] See ref *32*. To determine if solvent accessibility is affected by residue presence in protein binding surface, solvent accessible areas were compared in presence and absence of the partner protein. For Imm, Trp solvent-accessible area was also calculated in the X-ray structure of Imm alone (the X-ray structure of the individual C96 has not yet been reported) to detect conformation changes around Trp side chains. [b] From ref *32*. [c] From ref *31*.

V. Decreased Stability of the Cytotoxic Domain after Imm Release. The stability of isolated C96 compared to the C96Imm complex was probed using the temperature dependence of the amplitude of the CD signal at 228 nm (Figure 5B), discussed above (section III, Figure 4D) and previously described (*1*), and also of the intrinsic Trp fluorescence (Figure 5A). Thermal unfolding of C96 at pH 8.0 in 0.1 M NaCl measured by the change in ellipticity at 228 nm is characterized by a T_m of 47.0 ± 0.3 °C (Figure 5B). It is more stable in 1 M (T_m, 49.2 ± 0.4 °C) than in 10 mM NaCl (T_m, 46.0 ± 0.3 °C), implying that destabilizing repulsive electrostatic interactions prevail over attractive forces be-

[3] Elimination of a maximum at 226 nm in Y507A and Y519A mutants of C96 was previously reported to be a consequence of C96 unfolding, inferred from the loss of cooperative melting (*1*). The W498F and W509F mutations (Trp and Phe volume, 228 and 190 Å^3, respectively) generated in the present study did not eliminate cooperative thermal unfolding of C96.

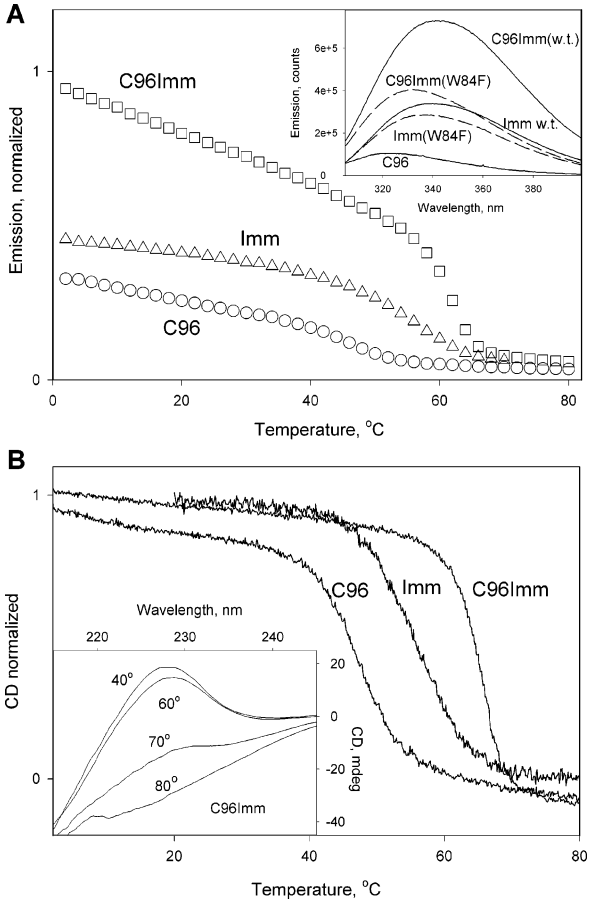

FIGURE 5: Imm removal results in decreased stability of C96. (A) Decreased stability ("melting") of C96 described by the temperature dependence of the fluorescence intensity of the two intrinsic Trp (W43 and W54 in C96 (Figure 1B), which corresponds to positions 498 and 509 in the intact protein). Melting was recorded at 320 nm for C96 (circles) and at 330 nm for the Imm mutant W84F (triangles) and C96Imm(W84F) complex (squares). Emission spectra (305−400 nm) excited at 295 nm were measured in the range 2−80 °C with a 2 °C step and temperature equilibration time of 2 min. Inset: Fluorescence emission spectra of C96, wild-type Imm, and their complex shown as solid lines. Spectra of Imm mutant W84F and its complex with C96 (dashed lines). Complexes were formed by mixing an equimolar amount of C96 and Imm at 20 °C. Conditions: excitation, 295 nm; protein concentration, 1 μM; buffer, 20 mM Tris, pH 8.0, and 0.1 M NaCl. (B) Temperature dependence of the amplitudes of CD at 228 nm. Melting curves were measured at 228 nm for C96 (T_m, 47.0 °C) and the C96Imm complex (T_m, 65.5 °C) and at 230 nm for Imm (T_m, 56.4 °C). Conditions: protein concentration, 3 μM; heating rate, 30 °C/h. (Inset) CD spectra of 50 μM C96Imm complex at 40, 60, 70, and 80 °C.

tween C96 side chains. Imm has a greater thermal stability (T_m, 56.4 ± 0.5 °C; Figure 5B). The melting of the C96Imm complex showed a single cooperative transition with a T_m of 65.5 ± 0.4 (Figure 5B). Thus, release of Imm from C96Imm resulted in a significant ($\Delta T_m = -18$ °C) decrease in the stability of C96.

For melting measured by Trp emission spectroscopy, the Imm W84F mutant was used to avoid an effect of local environment changes around W84 (Figure 1B).[4] Thermal unfolding for Imm alone and C96Imm shows single cooperative transitions characterized by a T_m of 57 ± 2 and 62 ± 2 °C, respectively (Figure 5A). The unfolding profile for C96 is biphasic (Figure 5A), with a noncooperative decrease in Trp fluorescence intensity below 40 °C and a cooperative

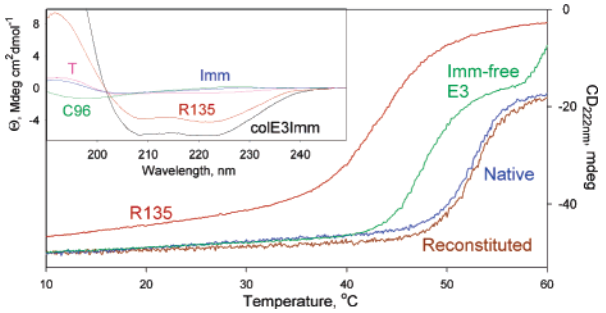

FIGURE 6: Decreased stability of the R-domain coiled coil of Imm-free colE3. Melting curves are shown for 2 μM Imm-free colE3 (T_m, 47.7 °C, green), coiled-coil R135 (T_m, 43.5 °C, red), native colE3Imm complex (T_m, 52.8 °C, blue), and an equimolar mixture of Imm-free colE3 and Imm (T_m, 52.6 °C, brown). (Inset) Far-UV CD spectra of recombinant fragments and the entire colE3Imm complex: T-domain (residues 84−315), pink; R135 (residues 313−447)-E-His_6, red; C96, GSHM (residues 455−551), green; Imm (residues 1−84), blue; colE3Imm complex, black. Specific molar ellipticity, Θ, was calculated per mole of polypeptide. Conditions: buffer, 10 mM Tris, pH 8.0, and 0.1 M NaCl; temperaure, 20 °C.

transition of small amplitude with T_m = 46 ± 2 °C, in agreement with the CD data (Figure 5B). The decreased T_m and cooperativity of melting are consistent with a relatively disordered structure of Imm-free C96.

VI. Imm Release Results in Decreased Stability of Coiled-Coil R135. The coiled-coil R-domain with 84% α-helix content (*8*) has a far-UV CD spectrum with large amplitude minima at 208 and 222 nm and a maximum at 192 nm (Figure 6, inset, red), which dominates the CD spectrum of colE3Imm (Figure 6, inset, black). The isolated R135 was characterized by a T_m of 43.8 ± 0.4 °C (Figure 6, red) compared to T_m = 52.4 ± 0.3 °C in the intact colE3Imm (Figure 6, blue). Removal of Imm resulted in a 5 °C decrease of the T_m of Imm-free colE3 to 47.7 ± 0.5 °C (Figure 6, green), showing a decrease in thermal stability of the R-domain coiled coil. Reconstitution of the colE3Imm complex by addition to Imm-free colE3 of an equimolar amount of Imm restored the thermal stability of the coiled coil, T_m = 52.6 ± 0.6 °C (Figure 6, brown).

DISCUSSION

The Elongate Structure of the colE3Imm Complex. The asymmetric colE3Imm complex (Figure 1A), in which the N-terminal translocation and the C-terminal cytotoxic domains (*8*) are on the one end of the colicin E3 molecule and the BtuB binding apex of the coiled-coil domain is on the other (*10*), has implications for the mechanism of cellular import of the colicin. The BtuB receptor binding site in colicin E3 is situated far from the TolB box, residues 34−46 (*37*, *38*), and an OmpF binding site, residues 5 and/or 7 (*21*). Both of these sites are located in the N-terminal 83-residue glycine-rich disordered segment of the translocation domain. This disorder can increase the cross section of BtuB-

[4] The formation of the C96Imm complex is associated with a significant increase in intrinsic Trp fluorescence intensity (*1*, *2*). Analysis of solvent accessibility of aromatic side chains in the crystallized C96Imm complex (Table 1) implies that the enhanced emission might arise from Trp84 of Imm. The Imm W84F mutant showed little enhancement of Trp fluorescence upon C96Imm complex formation (Figure 5A, inset), implying that W84 is primarily responsible for the enhancement.

bound colicin used to search for a second outer membrane protein, OmpF, which is utilized for import. The C-terminal cytotoxic domain is also located on the distal end of the colicin molecule relative to the BtuB binding site, connected to the translocation domain through the immunity protein. The implied function of the 100 Å long coiled coil of the R-domain, the stability of which is enhanced by its Ala-coil nature (*8*), is to capture OmpF, present at a high concentration ($\sim 10^5$ copies/cell) in the outer membrane (*39*), and to place the translocation domain in a position favorable for formation of a BtuB-colicin−OmpF translocon (*10*).

Imm−C96 Interaction. Crystallographic analysis of colicin E3 complexed with its cognate Imm protein (*8*, *32*) showed that a strong affinity between these proteins originates from multiple interactions between extended contact areas of Imm and the cytotoxic domain. Formation of a complex between C96 and Imm results in the loss of ≈2550 Å^2 of solvent-accessible area. Twenty-three water molecules in the vicinity of the contact areas are completely buried or have decreased accessibility (*32*). These water molecules bridge Imm to C96 via hydrogen bonds, or fill gaps, increasing the complementation of the interacting contact areas. The weaker but essential interactions of Imm with the colicin T-domain also contribute to the formation of a tight complex between colicin E3 and Imm.

The release of Imm from colicin in the course of anion-exchange chromatography was not anticipated and is attributed to strong electrostatic interaction of anionic Imm with the Q column at low ionic strength. These interactions induce conformation changes in the C96Imm complex that result in C96 release. We note that this method could be useful in studies of other high-affinity enzyme−inhibitor complexes.

The 10-residue N-terminal α-helix of C96 (*32*) is connected with the β-sheet subdomain through a long linker coil. Most of the linker coil and α-helix contact only Imm and do not contribute to the C96 hydrophobic core. Four long β-strands form an antiparallel β-sheet structure of C96 in the C96Imm complex, significant parts of which are buried and solvent-inaccessible, including W498 and W509. Superposition of the backbone atoms of C96 and Imm (Figure 1C) in crystal structures of the C96Imm complex (*32*), and in the entire colE3Imm complex (*8*), shows that the backbone of Imm is not significantly altered by contact with the T-domain (RMSD for backbone and all atoms, 0.36 and 0.96 Å, respectively), supporting the previous inference that Imm is a rigid molecule (*32*). A somewhat larger RMSD can be calculated for C96 (0.52 and 1.17 Å, respectively), although it does not interact with the T-domain in the entire colE3Imm, suggesting that the cytotoxic domain has a flexible structure that uses the rigid Imm contact surface as a template for its folding.

Extensively Unfolded State of Imm-free C96. Crystallographic data (Figure 1B), and analysis by Trp fluorescence and far- and near-UV CD spectra of bound and free forms of C96 and Imm (Figures 4 and 5), imply extensive unfolding of C96 after Imm removal. Thus, Imm must be removed to allow the unfolding of C96 that is necessary for its import. It is noted that although the CD spectroscopy is diagnostic of a mostly unfolded state, C96 is not completely unfolded, as Imm-free C96 retains a hydrophobic core. This is inferred from the blue-shifted Trp fluorescence emission spectrum and the presence of CD signals of a small amplitude in the near-UV region.

From studies on disulfide cross-linking of Cys-substituted mutants of OmpF (*40*), it was concluded that colicins could not be transferred through its pore. However, it is noted that (i) the presence of the L3 loop in the OmpF channel lumen resulted in a decrease in its cross section size to 7×11 Å (*15*), which would not necessarily prevent transfer of the unfolded polypeptide, and (ii) the successful cross-linking in this work was obtained only for Cys pairs located close to loop connection with the barrel which would not affect mobility of the loop apex. The latter inference is also supported by the lack of effect of cross-linking on voltage gating of OmpF Cys-substituted mutants (*41*).

Occlusion of OmpF. We consider the specific occlusion of OmpF by colicin domains (*21*) in the artificial planar bilayer to imply polypeptide insertion into OmpF channels and their transfer in vivo. It is presently not known whether the occlusion is an indicator of insertion into OmpF or of specific binding to the OmpF extracellular domain. The voltage dependence of the occlusion, dependence on side of colicin E3 addition, and the similar specific occlusion of TolC by colicin E1 and OmpF by colicin N (*21*) imply that the population of OmpF in the planar bilayer membrane is inserted with the extracellular side on the *trans*-side of the bilayer membrane and occlusion of OmpF by the colicin or its subdomains is an indicator of insertion.

Imm-free C96 added from the *trans*-side of the membrane efficiently occluded OmpF channels (Figure 3C,D), and C96 complexed with Imm did not occlude (Figure 3B). The requirement for OmpF occlusion of a *cis*-negative transmembrane potential implies that the *cis*-compartment relative to the planar bilayer corresponds to the periplasmic side of the *E. coli* outer membrane. The requirement of the *cis*-negative potential as a driving force for occlusion may be a consequence of the absence of BtuB in the planar bilayer in this in vitro assay. A *cis*-positive potential opens OmpF channels occluded by the C-domain (Figure 3C).

Thus, after formation of an OmpF−BtuB translocon, a process in which the colicin N-terminal translocation domain plays a key role, the C96 cytotoxic domain depleted of Imm could use one of the two channels of the OmpF trimer unoccupied by the T-domain to pass through the outer membrane into the periplasm.

Recruitment of OmpF to the BtuB−colE9 complex was detected (*14*) in a detergent extract using Ni^{2+}-chelation chromatography of Imm His-tagged at the C-terminus. Besides colE9, the complexes also contained BtuB and, while substoichiometric, a significant amount (0.3 ± 0.2 equiv) of OmpF. This would imply that Imm release is not necessary for formation of the BtuB−OmpF−colicin translocon. It has also been shown that unfolding of the coiled-coil termini is required for colicin import, as introduction of opposing cysteines into the coiled-coil R-domain of colicin E9, which allowed formation of a disulfide bond across the coiled coil, resulted in the elimination of colicin cytotoxicity (*42*). The OmpF recruitment to the BtuB−colicin complex measured by Housden et al. (*14*) in a "pull down" experiment was not prevented by the disulfide bond in the coiled coil of the ColE9. Thus, it can be inferred that the unfolded state is not required for binding to OmpF of the BtuB-bound colicin, presumably because the colicin has a permanently unfolded

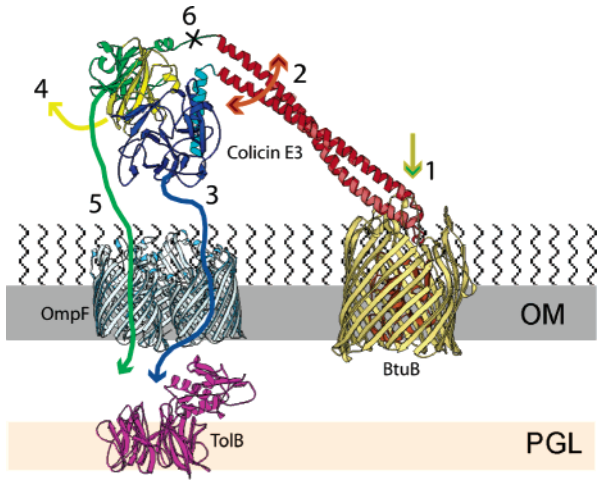

FIGURE 7: Sequence of molecular events in colicin E3 imports through the outer membrane BtuB/OmpF translocon: (1) colicin binding to BtuB; (2/3) partial unfolding of the R- and T-domains and OmpF recruitment into translocon through interaction of the T-domain N-terminus with OmpF; (4) Imm release; (5) C96 unfolding and insertion into the OmpF channel unoccupied by the T-domain; (6) proteolytic cleavage of colicin between the C- and R-domains (*45*).

N-terminus. Major unfolding of C96 and unmasking of the OmpF recognition site are, however, necessary for its binding to, and passage through, the 7 × 11 Å aperture of the OmpF pore. Unfolding of the termini of the coiled coil, associated with binding of the colicin E3 R-domain to BtuB, was documented in the crystal structure of the R135BtuB complex and by far-UV CD spectroscopy (*10*).

In conclusion, a proposal for the sequence of molecular events that delineate colicin E3 import into the periplasm would be initiated by colicin E3 binding to the BtuB receptor (Figure 7, step 1). Subsequently, structural changes and events would occur in the following approximate order: steps 2 and 3, OmpF is recruited through the extended coiled coil to form a BtuB−colicin−OmpF translocon through interaction of the N-terminal disordered T83 segment; step 4, the remainder of the T-domain is unfolded, Imm is released, and the C96 cytotoxic domain is unfolded; step 5, the unfolded cytotoxic domain inserts into the OmpF pore (probably through its C-terminus) and passes into the periplasm, where it would interact with the translocation apparatus (TolAQR) (*43*). Translocation of the cytotoxic domain across the periplasm and through the cytoplasm membrane that contains the translocation apparatus would be preceded (or followed if cleavage takes place in the periplasm) by a proteolytic cleavage (step 6) (*19*, *44*) as found between the R- and C-domains in colicin E7 (*45*). This cleavage would remove the constraint to movement of the cytotoxic domain that results from tight binding of the R-domain to BtuB (*46*).

REFERENCES

1. Walker, D., Lancaster, L., James, R., and Kleanthous, C. (2004) Identification of the catalytic motif of the microbial ribosome inactivating cytotoxin colicin E3, *Protein Sci. 13*, 1603−1611.
2. Walker, D., Moore, G. R., James, R., and Kleanthous, C. (2003) Thermodynamic consequences of bipartite immunity protein binding to the ribosomal ribonuclease colicin E3, *Biochemistry 42*, 4161−4171.
3. Holland, I. B. (1977) in *The specificity and action of animal, bacterial and plant toxins* (Cuatrecasas, P., Ed.) pp 99−127, Chapman and Hall, London.
4. Cramer, W. A., Heymann, J. B., Schendel, S. L., Deriy, B. N., Cohen, F. S., Elkins, P. A., and Stauffacher, C. V. (1995) Structure-function of the channel-forming colicins, *Annu. Rev. Biophys. Biomol. Struct. 24*, 611−641.
5. Braun, V., Patzer, S. I., and Hantke, K. (2002) Ton-dependent colicins and microcins: modular design and evolution, *Biochimie 84*, 365−380.
6. James, R., Penfold, C. N., Moore, G. R., and Kleanthous, C. (2002) Killing of *E. coli* cells by E group nuclease colicins, *Biochimie 84*, 381−389.
7. Wiener, M., Freymann, D., Ghosh, P., and Stroud, R. M. (1997) Crystal structure of colicin Ia, *Nature 385*, 461−464.
8. Soelaiman, S., Jakes, K., Wu, N., Li, C. M., and Shoham, M. (2001) Crystal structure of colicin E3: Implications for cell entry and ribosome inactivation, *Mol. Cell 8*, 1053−1062.
9. Zakharov, S. D., and Cramer, W. A. (2004) On the mechanism and pathway of colicin import across the *E. coli* outer membrane, *Front. Biosci. 9*, 1311−1317.
10. Kurisu, G., Zakharov, S. D., Zhalnina, M. V., Bano, S., Eroukova, V. Y., Rokitskaya, T. I., Antonenko, Y. N., Wiener, M. C., and Cramer, W. A. (2003) The structure of BtuB with bound colicin E3 R-domain implies a translocon, *Nat. Struct. Biol. 10*, 948−954.
11. Benedetti, H., Frenette, M., Baty, D., Lloubes, R., Geli, V., and Lazdunski, C. (1989) Comparison of the uptake systems for the entry of various BtuB groups colicins into *Escherichia coli*, *J. Gen. Microbiol. 135*, 3413−3420.
12. Rehling, P., Brandner, K., and Pfanner, N. (2004) Mitochondrial import and the twin-pore translocase, *Nat. Rev. Mol. Cel. Biol. 5*, 519−530.
13. Mokranjac, D., and Neupert, W. (2005) Protein import into mitochondria, *Biochem. Soc. Trans. 33*, 1019−1023.
14. Housden, N. G., Loftus, S. R., Moore, G. R., James, R., and Kleanthous, C. (2005) Cell entry mechanism of enzymatic bacterial colicins: Porin recruitment and the thermodynamics of receptor binding, *Proc. Natl. Acad. Sci. U.S.A. 102*, 13849−13854.
15. Cowan, S. W., Schirmer, T., Rumel, G., Steiert, M., Ghosh, R., Pauptit, R. A., Jansonius, J. N., and Rosenbusch, J. (1992) Crystal structures explain functional properties of two *E. coli* porins, *Nature 358*, 727−733.
16. Jeanteur, D., Schirmer, T., Fourel, D., Simonet, V., Rummel, G., Widmer, C., Rosenbusch, J. P., Pattus, F., and Pages, J. M. (1994) Structural and functional alterations of a colicin-resistant mutant of OmpF porin from *Escherichia coli*, *Proc. Natl. Acad. Sci. U.S.A. 91*, 10675−10679.
17. Kolade, O. O., Carr, S., Kuhlmann, U. C., Pommer, A., Kleanthous, C., Bouchcinsky, C., and Hemmings, A. M. (2002) Structural aspects of the inhibition of DNase and rRNase colicins by their immunity proteins, *Biochimie 84*, 439−446.
18. Graille, M., Mora, L., Buckingham, R. H., van Tilbeurgh, H., and de Zamaroczy, M. (2004) Structural inhibition of the colicin D tRNase by the tRNA-mimicking immunity protein, *EMBO J. 23*, 1474−1482.
19. Krone, W. J., de Vries, P., Koningstein, G., de Jonge, A. J., de Graaf, F. K., and Oudega, B. (1986) Uptake of cloacin DF13 by susceptible cells: removal of immunity protein and fragmentation of cloacin molecule, *J. Bacteriol. 166*, 260−268.
20. Jakes, K., and Zinder, N. D. (1974) Highly purified colicin E3 contains immunity protein, *Proc. Natl. Acad. Sci. U.S.A. 71*, 3380−3384.
21. Zakharov, S. D., Eroukova, V. Y., Rokitskaya, T. I., Zhalnina, M. V., Sharma, O., Loll, P. J., Zgurskaya, H. I., Antonenko, Y. N., and Cramer, W. A. (2004) Colicin occlusion of OmpF and TolC channels: outer membrane translocons for colicin import, *Biophys. J. 87*, 3901−3911.
22. Ohno, S., Ohno-Iwashita, Y., Suzuki, K., and Imahori, K. (1977) Purification and characterization of active component and active fragment of colicin E3, *J. Biochem. 82*, 1045−1053.
23. Mueller, P., Rudin, D. O., Tien, H. T., and Wescott, W. C. (1962) Reconstitution of cell membrane structure *in vitro* and its transformation into an excitable system, *Nature 194*, 979.
24. Jakes, K., Zinder, N. D., and Boon, T. (1974) Purification and properties of colicin E3 immunity protein, *J. Biol. Chem. 249*, 438−444.
25. Bowman, C. M., Sidikaro, J., and Nomura, M. (1971) Specific inactivation of ribosomes by colicin E3 *in vitro* and mechanism of immunity in colicinogenic cells, *Nat. New Biol. 234*, 133−137.

26. Levinson, B. L., Pickover, C. A., and Richards, F. M. (1983) Dimerization by colicin E3 in the absence of immunity protein, *J. Biol. Chem. 258*, 10967−10972.
27. Benz, R., Schmid, A., and Hancock, R. E. W. (1985) Ion selectivity of gram-negative bacterial porins, *J. Bacteriol. 162*, 722−727.
28. Alcaraz, A., Nestorovich, E. M., Aguilella-Arzo, M., Aguilella, V. M., and Bezrukov, S. M. (2004) Salting out the ionic selectivity of a wide channel: the asymmetry of OmpF, *Biophys. J. 87*, 943−957.
29. Tozawa, K., MacDonald, C. J., Penfold, C. N., James, R., Kleanthous, C., Clayden, N. J., and Moore, G. R. (2005) Clusters in an intrinsically disordered protein create a protein-binding site: the TolB-binding region of colicin E9, *Biochemistry 44*, 11496−11507.
30. Collins, E. S., Whittaker, S. B.-M., Tozawa, K., MacDonald, C., Boetzel, R., Penfold, C. N., Reilly, A., Clayden, N. J., Osborne, M. J., Hemmings, A. M., Kleanthous, C., James, R., and Moore, G. R. (2002) Structural dynamics of the membrane translocation domain of colicin E9 and its interaction with TolB, *J. Mol. Biol. 318*, 787−804.
31. Li, C., Zhao, D., Djebli, A., and Shoham, M. (1999) Crystal structure of colicin E3 immunity protein: an inhibitor of a ribosome-inactivating RNase, *Struct. Folding Des. 7*, 1365−1372.
32. Carr, S., Walker, D., James, R., Kleanthous, C., and Hemmings, A. M. (2000) Inhibition of a ribosome-inactivating ribonuclease: the crystal structure of the cytotoxic domain of colicin E3 in complex with its immunity protein, *Structure 8*, 949−960.
33. Venyaminov, S. Y., and Yang, J. T. (1996) in *Circular Dichroism and the Conformational Analysis of Biomolecules* (Fasman, G. D. E., Ed.) pp 581−603, Plenum, New York.
34. Venyaminov, S. Y., Baikalov, I. A., Shen, Z. M., Wu, C.-S. C., and Yang, J. T. (1993) Circular dichroic analysis of denatured proteins: inclusion of denatured proteins in the reference set, *Anal. Biochem. 214*, 17−24.
35. Chakrabartty, A., Kortemme, T., Padmanabhan, S., and Baldwin, R. L. (1993) Aromatic side-chain contribution to far-ultraviolet circular dichroism of helical peptides and its effect on measurement of helix propensities, *Biochemistry 32*, 5560−5565.
36. Woody, R. W., and Dunker, A. K. (1996) in *Circular dicroism and the Conformational Analysis of Biomolecules* (Fasman, G. D. E., Ed.) pp 109−157, Plenum Press, New York.
37. Bouveret, E., Rigal, A., Lazdunski, C., and Benedetti, H. (1997) The N-terminal domain of colicin E3 interacts with TolB which is involved in the colicin translocation step, *Mol. Microbiol. 23*, 909−920.
38. Hands, S. L., Holland, L. E., Vankemmelbeke, M., Fraser, L., Macdonald, C. J., Moore, G. R., James, R., and Penfold, C. N. (2005) Interactions of TolB with the translocation domain of colicin E9 require an extended TolB box, *J. Bacteriol. 187*, 6733−6741.
39. Nikaido, H. (2003) Molecular basis of bacterial outer membrane permeability revisited, *Microbiol. Mol. Biol. Rev. 67*, 593−656.
40. Bainbridge, G., Armstrong, G. A., Dover, L. G., Whelan, K. F., and Lakey, J. H. (1998) Displacement of OmpF loop 3 is not required for the membrane translocation of colicins N and A in vivo, *FEBS Lett. 432*, 117−122.
41. Bainbridge, G., Mobasheri, H., Armstrong, G. A., Lea, E. J. A., and Lakey, J. H. (1998) Voltage-gating of *Escherichia coli* porin: a cystein-scanning mutagenesis study of loop 3, *J. Mol. Biol. 275*, 171−176.
42. Penfold, C. N., Healy, B., Housden, N. G., Boetzel, R., Vankemmelbeke, M., Moore, G. R., Kleanthous, C., and James, R. (2004) Flexibility in the receptor-binding domain of the enzymatic colicin E9 is required for toxicity against *Escherichia coli* cells, *J. Bacteriol. 186*, 4520−4527.
43. Bouveret, E., Journet, L., Walburger, A., Cascales, E., Benedetti, H., and Lloubes, R. (2002) Analysis of the *Escherichia coli* Tol-Pal and TonB systems by periplasmic production of Tol, TonB, colicin, or phage capsid soluble domains, *Biochimie 84*, 413−421.
44. de Zamaroczy, M., and Buckingham, R. H. (2002) Importation of nuclease colicins into *E. coli* cells: endoproteolytic cleavage and its prevention by the immunity protein, *Biochimie 84*, 423−432.
45. Shi, Z., Chak, K.-F., and Yuan, H. S. (2005) Identification of an essential cleavage site in ColE7 required for import and killing of cells, *J. Biol. Chem. 280*, 24663−24668.
46. Taylor, R., Burgner, J. W., Clifton, J., and Cramer, W. A. (1998) Purification and characterization of monomeric *Escherichia coli* vitamin B_{12} receptor with high affinity for colicin E3, *J. Biol. Chem. 273*, 31113−31118.

BI060694+